Three-Dimensional Green's Functions in an Anisotropic Half-Space With General Boundary Conditions

E. Pan[1]
Structures Technology, Inc.
543 Keisler Drive,
Cary, NC 27511
Mem. ASME

This paper derives, for the first time, the complete set of three-dimensional Green's functions (displacements, stresses, and derivatives of displacements and stresses with respect to the source point), or the generalized Mindlin solutions, in an anisotropic half-space ($z>0$) with general boundary conditions on the flat surface $z=0$. Applying the Mindlin's superposition method, the half-space Green's function is obtained as a sum of the generalized Kelvin solution (Green's function in an anisotropic infinite space) and a Mindlin's complementary solution. While the generalized Kelvin solution is in an explicit form, the Mindlin's complementary part is expressed in terms of a simple line-integral over $[0,\pi]$. By introducing a new matrix **K**, *which is a suitable combination of the eigenmatrices* **A** *and* **B**, *Green's functions corresponding to different boundary conditions are concisely expressed in a unified form, including the existing traction-free and rigid boundaries as special cases. The corresponding generalized Boussinesq solutions are investigated in details. In particular, it is proved that under the general boundary conditions studied in this paper, the generalized Boussinesq solution is still well-defined. A physical explanation for this solution is also offered in terms of the equivalent concept of the Green's functions due to a point force and an infinitesimal dislocation loop. Finally, a new numerical example for the Green's functions in an orthotropic half-space with different boundary conditions is presented to illustrate the effect of different boundary conditions, as well as material anisotropy, on the half-space Green's functions.* [DOI: 10.1115/1.1532570]

Introduction

Green's functions (due to a concentrated source) are of great interests in both theoretical and applied mechanics ([1–3]). With increasing popularity of the integral equation method among different engineering fields, research on various Green's functions is increasing. The half-space Green's function alone has been applied in materials science ([4–6]), rock engineering ([7,8]), inverse problem [6], and contact mechanics ([9–12]). However, because of complexity, most three-dimensional half-space Green's functions are for the traction-free boundary condition only, including the isotropic half-space solution by Mindlin [13], transversely isotropic half-space solution by Pan and Chou [14], and anisotropic half-space solution by Willis [9], Barnett and Lothe [4], Barber and Sturla [15], Ting [2], Wu [16], and Pan and Yuan [17]. While the half-space Green's functions with a rigid surface can also be reduced from the corresponding bimaterial Green's functions, no Green's function solution exists in an anisotropic half-space with any mixed surface boundary conditions, with the exception of the transversely isotropic half-space Green's solution by Yu et al. [18] for the slippery boundary condition, which includes the isotropic solution of Dundurs and Hetenyi [19] as a special case.

While the traction-free and rigid boundary conditions on the surface of a half-space are perhaps the most common ones in engineering applications, the mixed boundary conditions, in particular the slippery condition, have been also used in various practical problems ([20,21]). For example, in rock and foundation engineering, the slippery boundary condition has been used to model a large-size soil deposit underlain by a hard bedrock base ([22]). In plate theory, the roller or simple supported condition resembles the slippery surface condition ([23]). The slippery condition has been also used to describe the connection between an ideal fluid and a solid in material science ([24]), and to model the bone implants in biomechanics ([25]).

Besides its applications in conventional engineering, Green's function method now becomes an essential tool in the numerical studies of strained semiconductor quantum devices where the strain-induced quantum dot growth in semiconductor nanostructures is crucial to the electronic performance ([26–28]). While under two-dimensional deformation, the strain-induced elastic and electric fields can be easily analyzed by the analytical solution of Ru ([29,30]), for those in the three-dimensional space, the Green's functions, as embedded in the Eshelby tensor ([5,31]), are required in the corresponding studies.

In Green's function solutions involving material anisotropy, the Stroh formalism has been shown to be mathematically elegant and technically powerful ([2,32,33]). Under two-dimensional deformation, Ting and co-workers ([2,34,35]) first derived the Green's functions in anisotropic half-plane with general boundary conditions. Two new eigenmatrices were introduced to replace the original eigenmatrices **A** and **B**, and the solution of the general boundary value problems was expressed in terms of a new single Stroh formalism ([2,34]). The general boundary conditions considered by Ting and co-workers ([2,34,35]) include, as special cases, the traction-free, rigid, and slippery boundary conditions, and their solution covers at least eight different sets of boundary conditions (to be defined later). While the two-dimensional deformation in terms of the Stroh formalism is relatively easy, the

[1]Currently at the Department of Civil Engineering, University of Akron, Akron, OH 44325-3905. e-mail: pan2@uakron.edu

Contributed by the Applied Mechanics Division of THE AMERICAN SOCIETY OF MECHANICAL ENGINEERS for publication in the ASME JOURNAL OF APPLIED MECHANICS. Manuscript received by the ASME Applied Mechanics Division, Feb. 19, 2001; final revision, Mar. 5, 2002. Associate Editor: D. A. Kouris. Discussion on the paper should be addressed to the Editor, Prof. Robert M. McMeeking, Department of Mechanical and Environmental Engineering, University of California–Santa Barbara, Santa Barbara, CA 93106-5070, and will be accepted until four months after final publication of the paper itself in the ASME JOURNAL OF APPLIED MECHANICS.

corresponding three-dimensional deformation is much more complicated. Although in recent years, the Stroh formalism was extended to certain three-dimensional Green's function solutions ([2,16,17]) no literature exists on generalizing the Stroh formalism to the three-dimensional problem with general boundary conditions.

In this paper, the author shows that, similar to the two-dimensional case, the Green's function in an anisotropic half-space with general boundary conditions can also be derived in terms of the extended Stroh formalism. The present study follows a recent development on three-dimensional Green's function solution in anisotropic bimaterials with perfectly bonded interface ([17]). It is found that, similar to the three-dimensional bimaterial case, the three-dimensional half-space Green's function with general boundary conditions can also be expressed as a sum of the generalized Kelvin Green's functions (the infinite-space Green's functions) and a Mindlin's complimentary part. While the former has an explicit expression ([36–39]), the latter can be expressed in terms of a simple line integral over $[0,\pi]$. Furthermore, a new matrix, named **K**, which is a suitable combination of the eigenmatrices **A** and **B**, is introduced so that the Green's functions corresponding to different boundary conditions can be concisely expressed in a unified form, including the existing traction-free and rigid boundaries as special cases. Also studied for the first time are the limit cases of the Green's functions when the source and/or field points are on the surface of the half-space with general boundary conditions. It is proved that even for these special cases, the corresponding Green's function solutions, the generalized Boussinesq solutions in particular, are still well defined. To enhance our understanding, a physical explanation for these solutions are also offered in terms of the equivalent concept of the Green's functions due to a point force and an infinitesimal dislocation loop. Finally, a new numerical example for the Green's functions in an orthotropic half-space with different boundary conditions is presented to illustrate the effect of different boundary conditions, as well as material anisotropy, on the half-space Green's functions.

In the following discussion, the three-dimensional Green's functions due to an interior point force in an anisotropic half-space with general boundary conditions will be also called the generalized Mindlin solutions. When the source point is located on the surface of the half-space, the corresponding Green's functions will be then called generalized Boussinesq solutions (i.e., the generalized surface Green's functions, see e.g., [4,15]. Also, by Green's functions, we mean the Green's displacements, stresses, and derivatives of displacements and stresses with respect to the source point.

Problem Description

Consider an anisotropic half-space occupying domain $x_3>0$ bounded by the $x_3=0$ plane. Let a point force $\mathbf{f}=(f_1,f_2,f_3)$ be applied in the half-space at source point $\mathbf{d}\equiv(d_1,d_2,d_3\equiv d)$ with $d_3>0$ and the field point be denoted by $\mathbf{x}\equiv(x_1,x_2,x_3\equiv z)$.[2] As usual, the problem domain is artificially divided into two regions: $z>d$ and $0\leqslant z<d$.

In the two regions of the half-space, the equations of equilibrium in terms of displacements u_k in the absence of body forces are written as

$$C_{ijkl}u_{k,lj}=0 \tag{1}$$

where C_{ijkl} is the elastic stiffness tensor of the half-space.

In this paper, the following eight different sets of boundary conditions on the surface $z=0$ ([2,34]) will be discussed. In other words, the half-space Green's functions are required to satisfy one of the eight sets of boundary conditions:

$$u_1=0;\ \ u_2=0;\ \ u_3=0 \tag{2a}$$

$$t_1=0;\ \ u_2=0;\ \ u_3=0 \tag{2b}$$

$$u_1=0;\ \ t_2=0;\ \ u_3=0 \tag{2c}$$

$$u_1=0;\ \ u_2=0;\ \ t_3=0 \tag{2d}$$

$$t_1=0;\ \ t_2=0;\ \ t_3=0 \tag{2e}$$

$$u_1=0;\ \ t_2=0;\ \ t_3=0 \tag{2f}$$

$$t_1=0;\ \ u_2=0;\ \ t_3=0 \tag{2g}$$

$$t_1=0;\ \ t_2=0;\ \ u_3=0 \tag{2h}$$

where the vector $\mathbf{t}(t_1,t_2,t_3)$ is the traction on the z=constant plane defined as

$$\mathbf{t}=(\sigma_{13},\sigma_{23},\sigma_{33}). \tag{3}$$

Similar to the corresponding two-dimensional analysis ([2,34]), we unify Equations (2*a–h*) by the following simple vector equation:

$$\mathbf{I}_u\mathbf{u}+\mathbf{I}_t\mathbf{t}=\mathbf{0} \tag{4}$$

where $\mathbf{I}_u$ and $\mathbf{I}_t$ are 3×3 diagonal matrices whose elements are either one or zero, and satisfy conditions

$$\mathbf{I}_u+\mathbf{I}_t=\mathbf{I};\quad \mathbf{I}_u\mathbf{I}_t=\mathbf{0} \tag{5}$$

with **I** being the unit matrix.

It is seen that Equations (2*a*) and (2*e*) corresponds to the rigid and traction-free boundary conditions, respectively, with $(\mathbf{I}_u,\mathbf{I}_t)=(\mathbf{I},\mathbf{0})$ and $(\mathbf{I}_u,\mathbf{I}_t)=(\mathbf{0},\mathbf{I})$. On the other hand, the slippery surface condition is represented by Equation (2*h*) and $\mathbf{I}_u=\mathrm{diag}[0,0,1]$ and $\mathbf{I}_t=\mathrm{diag}[1,1,0]$. We remark that instead of the displacement and stress function vectors $(\mathbf{u},\boldsymbol{\phi})$ adopted in the two-dimensional analysis ([2,34]), the displacement and traction vectors $(\mathbf{u},\mathbf{t})$ are used in this paper.

At the source level $z=d$ where the point force is applied, the displacement and traction vectors are required to satisfy the following conditions:

$$\mathbf{u}|_{z=d^-}=\mathbf{u}|_{z=d^+}$$
$$\mathbf{t}|_{z=d^-}-\mathbf{t}|_{z=d^+}=\delta(x_1-d_1)\,\delta(x_2-d_2)\mathbf{f} \tag{6}$$

along with the radiation condition so that the solution in the half-space vanishes as $|\mathbf{x}|$ approaches infinity.

Stroh Formalism in the Transformed Domain

To solve the problem described in the previous section, the two-dimensional Fourier transform (i.e., for the displacement)

$$\tilde{u}_k(y_1,y_2,z;\mathbf{d})=\int\int u_k(x_1,x_2,z;\mathbf{d})e^{iy_\alpha x_\alpha}dx_1dx_2 \tag{7}$$

is applied to Eq. (1). In Eq. (7), α takes the summation from 1 to 2.

A general solution to the Fourier transformed equation of (1) can be expressed as ([2,17])

$$\tilde{\mathbf{u}}(y_1,y_z,z;\mathbf{d}=\mathbf{a}e^{-ip\eta z} \tag{8}$$

with p and **a** satisfying the eigenrelation

$$[\mathbf{Q}+p(\mathbf{R}+\mathbf{R}^T)+p^2\mathbf{T}]\mathbf{a}=0. \tag{9}$$

The superscript T denotes matrix transpose, and

$$Q_{ik}=C_{ijks}n_jn_s,\ \ R_{ik}=C_{ijks}n_jm_s,\ \ T_{ik}=C_{ijks}m_jm_s \tag{10}$$

with

$$(n_1,n_2,n_3)\equiv(\cos\theta,\sin\theta,0)$$
$$(m_1,m_2,m_3)\equiv(0,0,1). \tag{11}$$

[2]Thereafter, the scalar variables z and d will be used exclusively for the third field coordinate x_3 and the third source coordinate d_3, respectively.

Note that a polar coordinate transform, defined below, has been used:

$$y_1 = \eta\cos\theta$$
$$y_2 = \eta\sin\theta. \tag{12}$$

It is observed that Eq. (9) is the Stroh eigenrelation for the oblique plane spanned by **n** and **m** defined in Eq. (11). It has been also shown (see i.e., [2]) that its eigenvalues are either complex or purely imaginary due to the positive requirement on the strain energy density.

Using the Stroh eigenvalues and the corresponding eigenvectors, the traction vector **t** on the z=constant plane and the in-plane stress vector **s**, namely

$$\mathbf{t} = (C_{13kl}u_{k,l}, C_{23kl}u_{k,l}, C_{33kl}u_{k,l}) \tag{13}$$

$$\mathbf{s} \equiv (\sigma_{11}, \sigma_{12}, \sigma_{22})$$
$$= (C_{11kl}u_{k,l}, C_{12kl}u_{k,l}, C_{22kl}u_{k,l}) \tag{14}$$

can be expressed in the Fourier-transformed domain as ([17])

$$\tilde{\mathbf{t}} = -i\eta\mathbf{b}e^{-ip\eta\zeta} \tag{15}$$

$$\tilde{\mathbf{s}} = -i\eta\mathbf{c}e^{-ip\eta\zeta} \tag{16}$$

with

$$\mathbf{b} = (\mathbf{R}^T + p\mathbf{T})\mathbf{a} = -\frac{1}{p}(\mathbf{Q} + p\mathbf{R})\mathbf{a}$$
$$\mathbf{c} = \mathbf{D}\mathbf{a}. \tag{17}$$

The matrix **D** is defined by

$$\mathbf{D} = \begin{bmatrix} C_{111\alpha}n_\alpha + pC_{1113} & C_{112\alpha}n_\alpha + pC_{1123} & C_{113\alpha}n_\alpha + pC_{1133} \\ C_{121\alpha}n_\alpha + pC_{1213} & C_{122\alpha}n_\alpha + pC_{1223} & C_{123\alpha}n_\alpha + pC_{1233} \\ C_{221\alpha}n_\alpha + pC_{2213} & C_{222\alpha}n_\alpha + pC_{2223} & C_{223\alpha}n_\alpha + pC_{2233} \end{bmatrix}. \tag{18}$$

If p_j, $\mathbf{a}_j$, and $\mathbf{b}_j$ $(j=1,2,...6)$ are the eigenvalues and the associated eigenvectors, we let

$$\mathrm{Im}p_j > 0,\ p_{j+3} = \overline{p_j},\ \mathbf{a}_{j+3} = \overline{\mathbf{a}_j},\ \mathbf{b}_{j+3} = \overline{\mathbf{b}_j},\ \mathbf{c}_{j+3} = \overline{\mathbf{c}_j}$$
$$(j=1,2,3)$$
$$\mathbf{A} = [\mathbf{a}_1, \mathbf{a}_2, \mathbf{a}_3],\ \mathbf{B} = [\mathbf{b}_1, \mathbf{b}_2, \mathbf{b}_3],\ \mathbf{C} = [\mathbf{c}_1, \mathbf{c}_2, \mathbf{c}_3] \tag{19}$$

where Im stands for the imaginary part and the overbar denotes the complex conjugate. It is further assumed that p_j are distinct and the eigenvectors $\mathbf{a}_j$, and $\mathbf{b}_j$ satisfy the following normalization relation:

$$\mathbf{b}_i^T\mathbf{a}_j + \mathbf{a}_i^T\mathbf{b}_j = \delta_{ij} \tag{20}$$

with δ_{ij} being the Kronecker delta.

It is worthwhile mentioning that should repeated eigenvalues occur, i.e., for transversely isotropic or isotropic materials, a slight perturbation on the material stiffness tensor would make them distinct with negligible error ([40]). Therefore, the unified and simple solution presented in this paper can be applied to materials with any material symmetry.

Half-Space Green's Functions in the Fourier Transformed Domain

For the anisotropic half-space, the general boundary conditions (4) on the surface $z=0$ and the condition (6) at the source level $z=d$, become, in the Fourier transformed domain, as

$$\mathbf{I}_u\tilde{\mathbf{u}} + \mathbf{I}_t\tilde{\mathbf{t}} = \mathbf{0} \tag{21}$$

and

$$\tilde{\mathbf{u}}|_{z=d^-} = \tilde{\mathbf{u}}|_{z=d^+}$$
$$\tilde{\mathbf{t}}|_{z=d^-} - \tilde{\mathbf{t}}|_{z=d^+} = \mathbf{f}e^{iy_\alpha d_\alpha}. \tag{22}$$

Using these conditions as well as the requirement that the solution should vanish as $|\mathbf{x}|$ approaches infinity, the half-space Green's function in the Fourier transformed domain can be derived as ([2,17]) follows:

For $0 \leqslant z < d$:

$$\tilde{\mathbf{u}}(y_1, y_2, z; \mathbf{d}) = i\eta^{-1}\mathbf{A}\langle e^{-ip_*\eta(z-d)}\rangle\mathbf{q}^\infty - i\eta^{-1}\overline{\mathbf{A}}\langle e^{-i\overline{p}_*\eta z}\rangle\mathbf{q}$$
$$\tilde{\mathbf{t}}(y_1, y_2, z; \mathbf{d}) = \mathbf{B}\langle e^{-ip_*\eta(z-d)}\rangle\mathbf{q}^\infty - \overline{\mathbf{B}}\langle e^{-\overline{p}_*\eta z}\rangle\mathbf{q} \tag{23}$$
$$\tilde{\mathbf{s}}(y_1, y_2, z; \mathbf{d}) = \mathbf{C}\langle e^{-ip_*\eta(z-d)}\rangle\mathbf{q}^\infty - \overline{\mathbf{C}}\langle e^{-i\overline{p}_*\eta z}\rangle\mathbf{q}.$$

For $z > d$:

$$\tilde{\mathbf{u}}(y_1, y_2, z; \mathbf{d}) = -i\eta^{-1}\overline{\mathbf{A}}\langle e^{-ip_*\eta(z-d)}\rangle\overline{\mathbf{q}}^\infty - i\eta^{-1}\overline{\mathbf{A}}\langle e^{-i\overline{p}_*\eta z}\rangle\mathbf{q}$$
$$\tilde{\mathbf{t}}(y_1, y_2, z; \mathbf{d}) = -\overline{\mathbf{B}}\langle e^{-ip_*\eta(z-d)}\rangle\overline{\mathbf{q}}^\infty - \overline{\mathbf{B}}\langle e^{-i\overline{p}_*\eta z}\rangle\mathbf{q} \tag{24}$$
$$\tilde{\mathbf{s}}(y_1, y_2, z; \mathbf{d}) = -\overline{\mathbf{C}}\langle e^{-ip_*\eta(z-d)}\rangle\overline{\mathbf{q}}^\infty - \overline{\mathbf{C}}\langle e^{-i\overline{p}_*\eta z}\rangle\mathbf{q}.$$

where

$$\mathbf{q}^\infty = \mathbf{A}^T\mathbf{f}e^{iy_\alpha d_\alpha} \tag{25}$$

and

$$\langle e^{-ip*\eta z}\rangle = diag[e^{-ip_1\eta z}, e^{-ip_2\eta z}, e^{-ip_3\eta z}]. \tag{26}$$

The complex vector **q** in Eqs. (23) and (24) is to be determined.

Motivated by the unified and elegant expression for the Green's function in an anisotropic half-plane with general boundary conditions ([2]), we have found that if we introduce a new matrix **K** defined as

$$\mathbf{K} = \mathbf{I}_u\mathbf{A} + \mathbf{I}_t\mathbf{B} \tag{27}$$

then the complex vector **q** for the eight different sets of boundary conditions (2*a*–*h*) can be expressed, in a single vector equation, as

$$\mathbf{q} = \overline{\mathbf{K}}^{-1}\mathbf{K}\langle e^{ip_*\eta d}\rangle\mathbf{A}^T\mathbf{f}e^{iy_\alpha d_\alpha}. \tag{28}$$

It is also observed that the new matrix **K**, like **A** and **B**, is independent of the radial variable η, an important feature to be used later. Equation (28) is a very surprising result and will be the key factor when deriving the physical-domain Green's functions.

Substituting Eq. (28) into Eqs. (23) and (24) gives the half-space Green's displacements and stresses in the Fourier transformed domain, which possess the following important features:

1. As discussed by Pan and Yuan [17], the first terms in Eqs. (23) and (24) are the Fourier transformed-domain Green's functions for a homogeneous and anisotropic full space. Inverse of these Green's functions, i.e., the physical-domain solution, has been obtained by Tewary [36], Ting and Lee [37], Sales and Gray [38], and Tonon et al. [39] in an explicit form. Therefore, the inverse Fourier transform needs to be carried out only for the second terms of the solution, which resemble the complementary part of the Mindlin solution ([13]).

2. These unified Fourier transformed-domain solutions (Eqs. (23) and (24)) include the eight different sets of the boundary conditions (2*a*–*h*). Thus, to solve for the Green's function in an anisotropic half-space with different boundary conditions, one only needs to assign the matrix **K** defined by Eq. (28) with the corresponding boundary conditions, a remarkably simple result parallel to its two-dimensional counterpart ([2]).

3. In deriving the Fourier transformed-domain solution, the matrix **K** has been assumed to be nonsingular. This can be proved following a procedure similar to the corresponding two-dimensional analysis ([2]).

Generalized Mindlin Solution

Having obtained the Green's functions in the Fourier transformed domain, we now apply the inverse Fourier transform to Eqs. (23) and (24). To handle the double infinite integrals, the

polar coordinate transform (12) is introduced so that the infinite integral with respect to the radial variable η can be carried out exactly. Thus, the final half-space Green's function in the physical domain, i.e., the generalized Mindlin solution, can be expressed as a sum of a Kelvin's part in an explicit form and a Mindlin's complementary part in terms of a line integral over $[0,2\pi]$. The integral for the latter can actually be further reduced to an integral over $[0,\pi]$. In what follows, we will use only the displacement solution to illustrate the derivation and list the final results for other Green's functions. Assumption will be also made that the source point **d** is interior to the half-space. The limit case, namely, the corresponding Boussinesq solution (when the source point **d** is on the surface) will be discussed later.

Applying the inverse Fourier transform, the Green's displacement in Eq. (24) becomes

$$\begin{aligned}\mathbf{u}(x_1,x_2,z;\mathbf{d}) = &-\frac{i}{4\pi^2}\int\int\{\eta^{-1}\overline{\mathbf{A}}\langle e^{-i\overline{p}_*\eta(z-d)}\rangle \\ &\times\overline{\mathbf{q}}^{\infty}e^{-i(x_\alpha-d_\alpha)y_\alpha}\}dy_1dy_2 \\ &-\frac{i}{4\pi^2}\int\int\{\eta^{-1}\overline{\mathbf{A}}\langle e^{-i\overline{p}_*\eta z}\rangle \\ &\times\mathbf{q}e^{-i(x_\alpha-d_\alpha)y_\alpha}\}dy_1dy_2. \end{aligned} \tag{29}$$

The first integral in Eq. (29) corresponds to the full-space Green's displacement that is already available in an explicit form ([36–39]). Consequently, the inverse transform needs to be carried out only for the second integral, or the complementary part. Denoting the full-space Green's function tensor by $\mathbf{U}^{\infty}(\mathbf{x};\mathbf{d})$ with its row and column indices corresponding to the displacement component and point-force direction, respectively, and introducing the polar coordinate transform (12), the half-space Green's displacement tensor can be rewritten as

$$\begin{aligned}\mathbf{U}(\mathbf{x};\mathbf{d}) = \mathbf{U}^{\infty}(\mathbf{x};\mathbf{d}) &- \frac{i}{4\pi^2}\int_0^{2\pi}d\theta\int_0^{\infty}\overline{\mathbf{A}}\langle e^{-i\overline{p}_*\eta z}\rangle \\ &\times\overline{\mathbf{K}}^{-1}\mathbf{K}\langle e^{ip_*\eta d}\rangle e^{-i\eta[(x_1-d_1)\cos\theta+(x_2-d_2)\sin\theta]}\mathbf{A}^T d\eta. \end{aligned} \tag{30}$$

Since the matrices **A** (also **B** and **C**) and $\overline{\mathbf{K}}^{-1}\mathbf{K}$ are independent of the radial variable η, integral with respect to η can therefore be performed analytically, resulting in the following compact form:

$$\mathbf{U}(\mathbf{x};\mathbf{d}) = \mathbf{U}^{\infty}(\mathbf{x};\mathbf{d}) + \frac{1}{2\pi^2}\int_0^{\pi}\overline{\mathbf{A}}\mathbf{G}_1\mathbf{A}^{\mathbf{T}}d\theta \tag{31}$$

where[3]

$$(\mathbf{G}_1)_{ij} = \frac{(\overline{\mathbf{K}}^{-1}\mathbf{K})_{ij}}{-\overline{p}_i z + p_j d - [(x_1-d_1)\cos\theta+(x_2-d_2)\sin\theta]}. \tag{32}$$

It is noticed that the integral interval in Eq. (31) has been reduced from $[0,2\pi]$ to $[0,\pi]$ based upon certain properties of the integrand as a function of θ ([41]), plus a new relation for the matrix $\mathbf{K}^{-1}\mathbf{K}$, i.e., $\overline{\mathbf{K}}^{-1}\mathbf{K}(\theta+\pi) = -\mathbf{K}^{-1}\overline{\mathbf{K}}(\theta)$. Similar properties have also been used to derive the Green's stresses, derivatives of Green's displacements and stresses.

Following a similar procedure, the half-space Green's stress tensors can be derived and the results are listed as

$$\mathbf{T}(\mathbf{x};\mathbf{d}) = \mathbf{T}^{\infty}(\mathbf{x};\mathbf{d}) + \frac{1}{2\pi^2}\int_0^{\pi}\overline{\mathbf{B}}\mathbf{G}_2\mathbf{A}^T d\theta \tag{33a}$$

$$\mathbf{S}(\mathbf{x};\mathbf{d}) = \mathbf{S}^{\infty}(\mathbf{x};\mathbf{d}) + \frac{1}{2\pi^2}\int_0^{\pi}\overline{\mathbf{C}}\mathbf{G}_2\mathbf{A}^T d\theta. \tag{33b}$$

[3]Thereafter, the indices i and j take the range from 1 to 3.

In Eqs. (33*a*) and (33*b*), $\mathbf{T}^{\infty}(\mathbf{x};\mathbf{d})$ and $\mathbf{S}^{\infty}(\mathbf{x};\mathbf{d})$ are the full-space Green's stress tensors ([39]), and

$$(\mathbf{G}_2)_{ij} = \frac{(\overline{\mathbf{K}}^{-1}\mathbf{K})_{ij}}{\{-\overline{p}_i z + p_j d - [(x_1-d_1)\cos\theta+(x_2-d_2)\sin\theta]\}^2}. \tag{34}$$

Derivatives of the Green's displacements and stresses (tensors) with respect to the source point (d_1,d_2,d_3) are found to be

$$\frac{\partial\mathbf{U}(\mathbf{x};\mathbf{d})}{\partial d_j} = \frac{\partial\mathbf{U}^{\infty}(\mathbf{x};\mathbf{d})}{\partial d_j} - \frac{1}{2\pi^2}\int_0^{\pi}\overline{\mathbf{A}}\mathbf{G}_2\langle g_j\rangle\mathbf{A}^T d\theta \tag{35}$$

$$\begin{aligned}\langle g_1\rangle &= diag[\cos\theta,\cos\theta,\cos\theta] \\ \langle g_2\rangle &= diag[\sin\theta,\sin\theta,\sin\theta] \\ \langle g_3\rangle &= diag[p_1,p_2,p_3]\end{aligned} \tag{36}$$

$$\frac{\partial\mathbf{T}(\mathbf{x};\mathbf{d})}{\partial d_j} = \frac{\partial\mathbf{T}^{\infty}(\mathbf{x};\mathbf{d})}{\partial d_j} - \frac{1}{2\pi^2}\int_0^{\pi}\overline{\mathbf{B}}\mathbf{G}_3\langle g_j\rangle\mathbf{A}^T d\theta \tag{37a}$$

$$\frac{\partial\mathbf{S}(\mathbf{x};\mathbf{d})}{\partial d_j} = \frac{\partial\mathbf{S}^{\infty}(\mathbf{x};\mathbf{d})}{\partial d_j} - \frac{1}{2\pi^2}\int_0^{\pi}\overline{\mathbf{C}}\mathbf{G}_3\langle g_j\rangle\mathbf{A}^T d\theta \tag{37b}$$

$$(\mathbf{G}_3)_{ij} = \frac{(\overline{\mathbf{K}}^{-1}\mathbf{K})_{ij}}{\{-\overline{p}_i z + p_j d - [(x_1-d_1)\cos\theta+(x_2-d_2)\sin\theta]\}^3}. \tag{38}$$

Equations (31), (33), (35), and (37) are the *complete* Green's functions in an anisotropic half-space with general boundary conditions, or the generalized Mindlin solutions. It is emphasized that these Green's functions are presented in a unified and very simple form so that the eight different sets of the boundary conditions (2*a–h*) are all included. To find the Green's functions for a given set of boundary conditions, one only needs to assign the corresponding **K** matrix. For example, for $\mathbf{K}=\mathbf{B}$, the present half-space Green's displacements and stresses will then reduce to the existing solution ([2,4,16,17]) for the traction-free boundary condition case. Since the present solution includes all the eight different sets of the boundary conditions, it is therefore particularly convenient when investigating the effect of different boundary conditions on the problem solution based on the Green's function method.

Considering the complexity of the problem and yet the simplicity of the final physical-domain Green's function expressions for all the eight sets of the boundary conditions, it is seen that, by resorting to the Mindlin's superposition approach, the extended (three-dimensional) Stroh formalism is indeed a very powerful and elegant method. A direct application of the Fourier transform method, without employing the Stroh formalism, would require three-dimensional Fourier inverse integrals for the infinite Green's function, and four-dimensional Fourier inverse integrals for the complementary part ([42]).

Besides their concise expressions, the present half-space Green's functions (generalized Mindlin solutions) also possess the following important features:

1. Similar to the bimaterial Green's functions with perfectly bonded interface ([17]), the half-space Green's displacements, stresses and derivatives of displacements, and derivatives of stresses are inversely proportional to, respectively, a linear, quadratic, and cubic combination of the field and source coordinates. This feature resembles the behavior of the full-space Green's displacements ($\propto 1/r$), stresses and derivatives of displacements ($\propto 1/r^2$), and derivatives of stresses ($\propto 1/r^3$), with r being the distance between the source and field points.

2. Different to either the bimaterial Green's functions with perfectly bonded interface or the half-space Green's functions with traction-free boundary conditions (2*e*) where the source point **d**

can directly approach the interface or the surface for all the three point-force directions, the half-space Green's functions with other seven sets of boundary conditions need special attention when approaching the surface, a very interesting feature to be discussed in the next section.

3. Since the source point is not on the surface of the half-space (i.e., $d \neq 0$), the integrals in Eqs. (31), (33), (35), and (37) for performing the complementary part of the half-space Green's functions are regular and thus can be easily carried out by a standard numerical integral method such as the Gauss quadrature.

Generalized Boussinesq Solution

In the previous section, we derived the generalized Mindlin solution in an anisotropic half-space with general boundary conditions (2*a*–*h*). While the field point **x** can be anywhere in the half space, the source point **d** is assumed to be interior to the half-space (i.e., $d \neq 0$). We recall that in the Mindlin solution ([13]) to an isotropic half-space with traction-free boundary conditions, both field and source points (**x** and **d**) can be arbitrary, and the corresponding Boussinesq solution (for a point force in any direction on the surface; see, [43]) can be directly reduced from Mindlin solution by taking the source point to the surface (i.e., $d=0$). Furthermore, the special half-space surface Green's function where the field and source points are both on the surface (i.e., $z=0$ and $d=0$), can also be obtained either from Mindlin solution with $z=0$ and $d=0$ for from Boussinesq solution with $z=0$. Actually, this feature also holds for the Mindlin solution in a transversely isotropic ([14]) and general anisotropic half-space ([2,4,15–17]). It is important at this point to emphasize that this feature is based upon the condition that the surface of the half-space is traction-free (i.e., Eq. (2*e*)). Then, it is natural to ask the question: Can one safely take the source point to the surface (i.e., $d=0$) in the generalized Mindlin solution to obtain the corresponding generalized Boussinesq solution? The answer is yes!

First, it is observed that if the *i*-th component of the traction vector is zero (i.e., $t_i=0$) on the surface, with boundary conditions in other two directions being properly given, then the corresponding generalized Boussinesq solution exists for a surface point force acting in the *i*th direction. Furthermore, this solution can be directly obtained from the generalized Mindlin solution by letting $d=0$. We point out that the field point is assumed to be interior to the half-space (i.e., $z \neq 0$), leaving the case of $d=0$ and $z=0$ being treated separately in the next section. It is very interesting that Boussinesq (see [43]) derived solutions in an isotropic half-space subjected to two general types of boundary conditions to which the present boundary condition sets (2*d*) and (2*h*) have direct connection. Therefore, for example, for the boundary condition set (2*d*), the generalized Boussinesq solution to a normal point force (i.e., in the x_3-direction) on the surface with fixed tangential displacements (i.e., $u_1=0$ and $u_2=0$) is well-defined and can be directly reduced from the generalized Mindlin solution by taking $d=0$.

Now, let us examine the case where the *i*th component of the displacement vector is zero (i.e., $u_i=0$) on the surface, which is also subjected to a surface point force in the *i*th direction at the origin. Since the displacement component $u_i=0$ is described on the whole surface while a concentrated traction component $t_i(=-\delta(\mathbf{x}))$ is also given at the surface point $\mathbf{x}=(0,0,0)$, the resulting boundary condition is over imposed at $\mathbf{x}=(0,0,0)$! However, if we release the displacement condition at $\mathbf{x}=(0,0,0)$ for u_i, due to the fact that this is a concentrated force at $\mathbf{x}=(0,0,0)$, then the boundary value problem will be well defined. Actually, from a mathematical point of view, i.e., from Eqs. (31)–(38), it can be proved that when $d=0$, these Boussinesq solutions are still well defined and regular as long as $z \neq 0$. It is noted that the first terms in Eqs. (31), (33), (35), and (37) are the infinite-space Green's functions that are regular and become singular if and only if the field and source points are coincident to each other (i.e., $\mathbf{x}=\mathbf{d}$). The second terms in these equations are proportional to one of the $\mathbf{G}_i$ matrices defined by Eqs. (32), (34), and (38), which are again regular and well defined. Therefore, in conclusion, the generalized Boussinesq solutions with general boundary conditions are still well defined and regular (if $z \neq 0$).

To enhance our understanding, we now offer a physical explanation to the generalized Boussinesq solutions in terms of the equivalent concept of the Green's functions due to a point force and an infinitesimal dislocation loop. Using the Betti's reciprocity, it can be shown ([44–46]) that the following important equivalent between the Green's function of a unit point force and that of a unit infinitesimal dislocation loop holds (in a dimensionless form):

$$u_j^{uik}(\mathbf{d};\mathbf{x}) = \sigma_{ik}^{fj}(\mathbf{x};\mathbf{d}) \tag{39}$$

While the right-hand side of Eq. (39) denotes the Green's stress component (i,k) at the field point **x** due to a point force in the *j*th direction at **d**, the left-hand side denotes the displacement in the *j*th direction at the field point **d** due to an infinitesimal dislocation loop, with index (i,k) for the dislocation direction and the normal of the dislocation plane, at the source point **x**. Therefore, the stress field due to a point force can be equivalently considered as a displacement field due to an infinitesimal dislocation loop. The latter is well defined with an apparent physical meaning: The displacement response on the surface of the half-space **d** (since $d=0$) due to an interior infinitesimal dislocation loop at the source point **x** (since $z \neq 0$). A very interesting consequence of Eq. (39) is that if the boundary condition is rigid (2*a*), then the stress field within the whole half-space, due to a point force in any direction on the surface, is zero! Furthermore, our numerical tests have shown that for such a case, the displacement field is indeed zero. The only nonzero components are the derivatives of the displacement and stress with respect to the third source coordinate *d*. While whether or not this special Boussinesq solution (with rigid boundary condition) has any application is unknown to the author, it is worth mentioning that these numerically obtained features on the displacements, stresses, and derivatives of displacements and stresses are consistent with those in the corresponding two-dimensional half-plane ([2]) where analytical solutions exist.

Yet, another limit case is when the field and source points are both on the surface (i.e., $z=d=0$). The corresponding response is a special case of the surface Green function, and it is discussed and presented in the following section.

Special Surface Green's Function

When both the field and source points are on the surface (i.e., $z=d=0$), the half-space Green's functions are reduced (from either the generalized Mindlin or Boussinesq solutions) to a particular class of Green's functions called special surface Green's functions. Similar to the generalized Mindlin or Boussinesq solutions, these special surface Green's functions can be expressed as a sum of the generalized Kelvin solution in an explicit form and a Mindlin's complementary part. For the complementary part, however, the involved one-dimensional integral becomes singular and exists only in the sense of finite-part principle value ([47–49]). Assuming that the field and source coordinates on the surface are (x_1,x_2) and (d_1,d_2), respectively, and expressing their relative position in terms of the polar coordinate as $x_1-d_1=r\cos\theta_0$; $x_2-d_2=r\sin\theta_0$, then these special surface Green's functions are obtained as ([50])

$$\mathbf{U}(\mathbf{x};\mathbf{d}) = \mathbf{U}^{\infty}(\mathbf{x};\mathbf{d}) - \frac{1}{2\pi r}\left\{\frac{1}{\pi}\int_0^{\pi}\frac{\overline{\mathbf{AK}}^{-1}\mathbf{K}\mathbf{A}^T}{\cos(\theta-\theta_0)}d\theta + i[\overline{\mathbf{AK}}^{-1}\mathbf{K}\mathbf{A}^T]_{\theta=\theta_0+\pi/2}\right\} \tag{40}$$

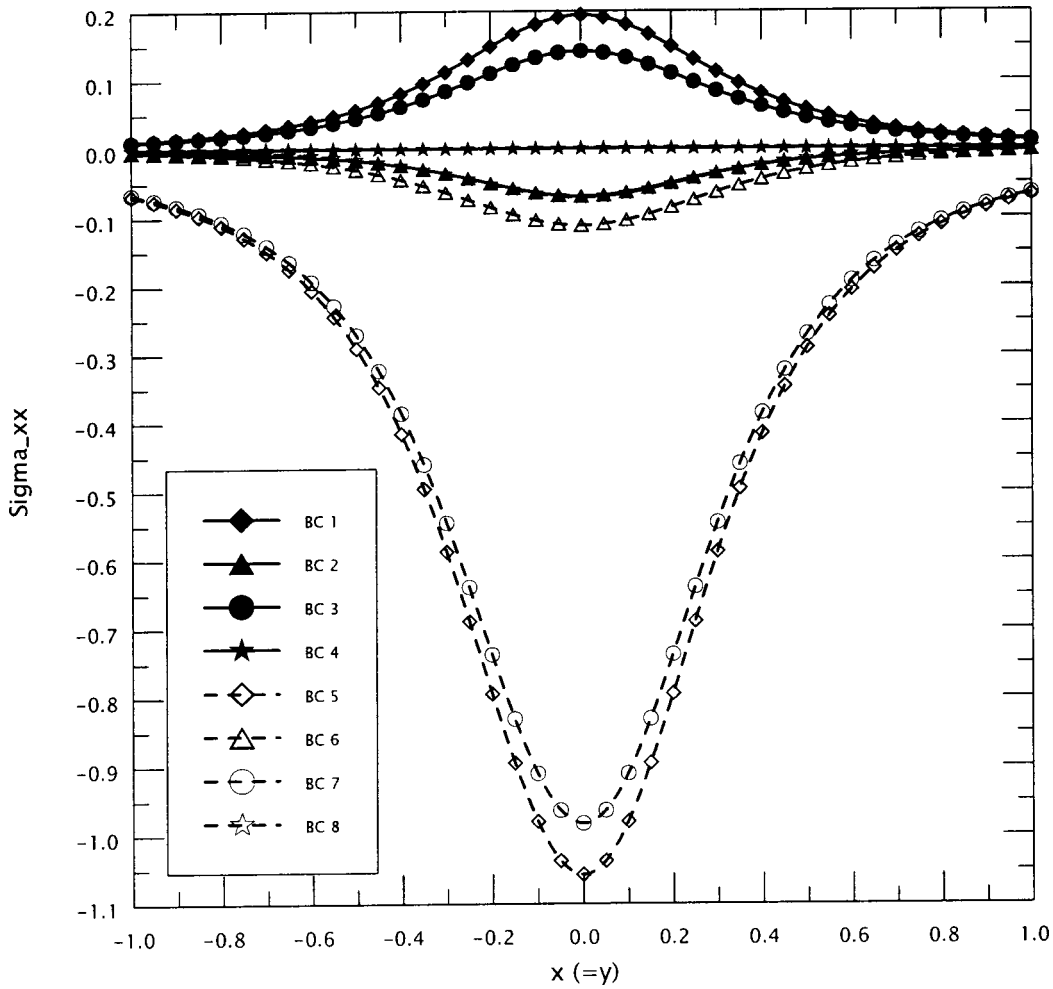

Fig. 1 Variation of in-plane stress component σ_{xx} along the line $x=y$ on the surface $z=0$, caused by the point force f=(0,0,1) and d=(0,0,1). Labels BC 1 to BC 8 correspond to the eight different sets of boundary conditions (2*a*–*h*).

$$\frac{\partial \mathbf{U}(\mathbf{x};\mathbf{d})}{\partial d_j}=\frac{\partial \mathbf{U}^{\infty}(\mathbf{x};\mathbf{d})}{\partial d_j}-\frac{1}{2\pi r^2}\left\{\frac{1}{\pi}\int_0^{\pi}\frac{\overline{\mathbf{AK}}^{-1}\mathbf{K}\langle g_j\rangle\mathbf{A}^T}{\cos^2(\theta-\theta_0)}d\theta-i\frac{d[\overline{\mathbf{AK}}^{-1}\mathbf{K}\langle g_j\rangle\mathbf{A}^T]}{d\theta}\bigg|_{\theta=\theta_0+\pi/2}\right\} \tag{41}$$

$$\mathbf{T}(\mathbf{x};\mathbf{d})=\mathbf{T}^{\infty}(\mathbf{x};\mathbf{d})+\frac{1}{2\pi r^2}\left\{\frac{1}{\pi}\int_0^{\pi}\frac{\overline{\mathbf{BK}}^{-1}\mathbf{K}\mathbf{A}^T}{\cos^2(\theta-\theta_0)}d\theta-i\frac{d[\overline{\mathbf{BK}}^{-1}\mathbf{K}\mathbf{A}^T}{d\theta}\bigg|_{\theta=\theta_0+\pi/2}\right\} \tag{42}$$

$$\frac{\partial \mathbf{T}(\mathbf{x};\mathbf{d})}{\partial d_j}=\frac{\partial \mathbf{T}^{\infty}(\mathbf{x};\mathbf{d})}{\partial d_j}+\frac{1}{2\pi r^3}\left\{\frac{2}{\pi}\int_0^{\pi}\frac{\overline{\mathbf{BK}}^{-1}\mathbf{K}\langle g_j\rangle\mathbf{A}^T}{\cos^3(\theta-\theta_0)}d\theta+i\left[\frac{d^2[\overline{\mathbf{BK}}^{-1}\mathbf{K}\langle g_j\rangle\mathbf{A}^T]}{d^2\theta}+[\overline{\mathbf{BK}}^{-1}\mathbf{K}\langle g_j\rangle\mathbf{A}^T]\right]\bigg|_{\theta=\theta_0+\pi/2}\right\} \tag{43}$$

$$\mathbf{S}(\mathbf{x};\mathbf{d})=\mathbf{S}^{\infty}(\mathbf{x};\mathbf{d})+\frac{1}{2\pi r^2}\left\{\frac{1}{\pi}\int_0^{\pi}\frac{\overline{\mathbf{CK}}^{-1}\mathbf{K}\mathbf{A}^T}{\cos^2(\theta-\theta_0)}d\theta-i\frac{d[\overline{\mathbf{CK}}^{-1}\mathbf{K}\mathbf{A}^T]}{d\theta}\bigg|_{\theta=\theta_0+\pi/2}\right\} \tag{44}$$

$$\frac{\partial \mathbf{S}(\mathbf{x};\mathbf{d})}{\partial d_j}=\frac{\partial \mathbf{S}^{\infty}(\mathbf{x};\mathbf{d})}{\partial d_j}+\frac{1}{2\pi r^3}\left\{\frac{2}{\pi}\int_0^{\pi}\frac{\overline{\mathbf{CK}}^{-1}\mathbf{K}\langle g_j\rangle\mathbf{A}^T}{\cos^3(\theta-\theta_0)}d\theta+i\left[\frac{d^2[\overline{\mathbf{CK}}^{-1}\mathbf{K}\langle g_j\rangle\mathbf{A}^T]}{d^2\theta}+[\overline{\mathbf{CK}}^{-1}\mathbf{K}\langle g_j\rangle\mathbf{A}^T]\right]\bigg|_{\theta=\theta_0+\pi/2}\right\}. \tag{45}$$

Several features regarding to the special surface Green's functions with general boundary conditions are observed:

1. Similar to the interfacial Green's functions in anisotropic bimaterial with perfectly bonded interface ([50]), the surface displacements, stresses and derivatives of displacements, and derivatives of stresses are inversely proportional, respectively, to r, r^2, and r^3, where r is the distance between the field and source points on the surface ($z=d=0$), a generalized consequence of self-

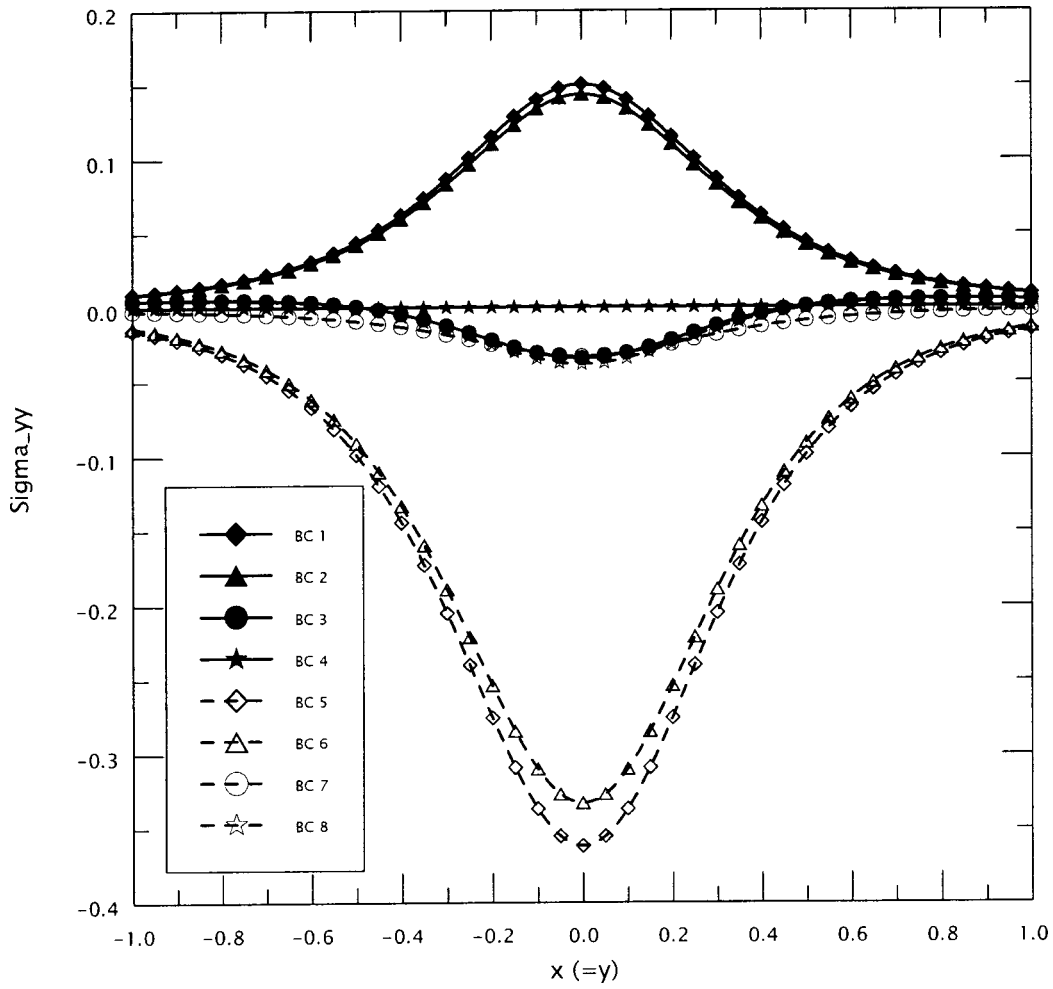

Fig. 2 Variation of in-plane stress component σ_{yy} along the line $x=y$ on the surface $z=0$, caused by the point force f=(0,0,1) at d=(0,0,1). Labels BC 1 to BC 8 correspond to the eight different sets of boundary conditions (2*a*–*h*).

similarity [9,15]. For the special surface Green's function component which is inversely proportional to r, r^2, and r^3, the corresponding finite-part integral has singular order of one ($1/\cos\theta$), two ($1/\cos^2\theta$), and three ($1/\cos^3\theta$), respectively; therefore, the special surface Green's functions are completely determined by the values on a unit circle on the surface $z=d=0$ (with field point on the unit circle and source point at the center of the circle). The finite-part integrals can be carried out accurately and efficiently using an adaptive scheme proposed recently by Pan and Yang [50].

2. For the traction-free boundary conditions (2*e*), the corresponding special surface Green's function was discussed previously by Willis [9], Barnett and Lothe [4], Barber and Sturla [15], Ting [2], Wu [16], and Pan and Yuan [17]. Even for this case, the complete special surface Green's functions are not available in the literature until very recently ([50]).

3. All the special surface Green's functions corresponding to the boundary conditions (2*a*–*d*) and (2*f*–*h*) are new.

Numerical Examples

For an anisotropic half space with general boundary conditions (2*a*–*h*), no previous solution is available except for the traction-free (2*e*) and rigid (2*a*) cases. While for the former, the Green's displacements and stresses were studied previously by Barrett and Lothe [4], Tine [2], Wu [16], and Pan and Yuan [17], the Green's functions for the latter can be numerically reduced from the bimaterial Green's functions of Pan and Yuan [17] for a perfectly bonded interface by letting the elastic tensor C_{ijkl} in the $z<0$ half-space being much stiffer than that in the concerned half-space region $z>0$. Although the isotropic ([19]) and transversely isotropic ([18]) half-space Green's solutions were studied before for the slippery surface boundary conditions (2*h*), no numerical result is available. Nevertheless, the present generalized Mindlin solutions have been self-checked for the boundary conditions (2*a*) and (2*e*), and for two of the mixed boundary conditions, namely conditions (2*d*) and (2*h*), to be discussed below.

Boussinesq (see [43]) derived the solution in an isotropic half-space when its boundary is subjected to two general types of boundary conditions: namely, the normal traction t_z and tangential displacements (u_x and u_y), and normal displacement u_z and tangential tractions (t_x and t_y). If, for the former, we assume a unit normal point force at the original and let the tangential displacements be zero (i.e., $u_x=u_y=0$), then the dilatation at any field point $\mathbf{x}=(x,y,z)$ of the half-space caused by this normal point force is found to be

$$\Delta=u_{i,i}=\frac{-z}{2\pi(\lambda+2\mu)(x^2+y^2+z^2)^{3/2}} \tag{46}$$

where λ and μ are the two Lame constants.

Similarly, for the latter, if we assume a unit point force in the x-direction at the original, traction-free in the y-direction (t_y

Table 1 Reduced and normalized stiffness matrix C_{ij} in the half-space

1.0352019	.0523837	.0523837	.0	.0	.0
	.1153771	.0405268	.0	.0	.0
		.1153771	.0	.0	.0
			.0333333	.0	.0
				.0333333	.0
					.0333333

$=0$), and zero-displacement in the z-direction ($u_z=0$), then the dilatation at any field point $\mathbf{x}=(x,y,z)$ of the half-space caused by this tangential point force is obtained as

$$\Delta = u_{i,i} = \frac{-x}{2\pi(\lambda+2\mu)(x^2+y^2+z^2)^{3/2}}. \tag{47}$$

It is seen that while Boussinesq solution (46) corresponds to the present Green's function with boundary condition (2*d*), solution (47) corresponds to that with the boundary condition (2*h*). For the former, the point force is in the z-direction and for the latter it is in the x-direction.

In the numerical testing, a Young's modulus $E=2.6$ and Poisson's ratio $\nu=0.3$ were assumed for the isotropic half-space. For the field point at $(x,y,z)=(1/\sqrt{3},1/\sqrt{3},1/\sqrt{3})$, both Eqs. (46) and (47) give the same dilatation value $\Delta=-0.026254$, while that predicted by the present Green's function solutions for the two cases is $\Delta=-0.026251$. This result not only has validated some of the present Green's functions, but also has shown that even the isotropic case can be easily handled by the present Stroh formalism using a slightly perturbed elastic property ([40]). For instance, to use the present Stroh formalism for the isotropic material, an orthotropic material was assumed with one of the three Poisson's ratios being perturbed to $\nu=0.2999$ while the other two being kept at $\nu=0.3$.

Next, the effect of different boundary conditions as well as material anisotropy, on the surface stress field is studied for an orthotropic half-space. The stiffness matrix (in its reduced and normalized form) from Pan and Yang [50] is given in Table 1. For this example, the source is fixed at $\mathbf{d}=(0,0,1)$ while the field point varies on the surface of the half-space as $\mathbf{x}=(x,x,0)$, with $\mathbf{x}\in[-1,1]$. While Figs. 1 and 2 show the variation of the normal stresses σ_{xx} and σ_{yy} caused by a unit point force in the z-direction, Figs. 3 and 4 show the variation of these normal stresses (σ_{xx} and σ_{yy}) due to a unit point force in the x-direction. In these figures, results for the eight different sets of boundary conditions (2*a*–*h*) are labeled as BC 1 and BC 8, respectively. These numerical results are believed to be new and possess the following interesting features:

1. For the given material (orthotropic), the surface normal stresses σ_{xx} and σ_{yy} are either symmetric (Figs. 1 and 2) or anti-

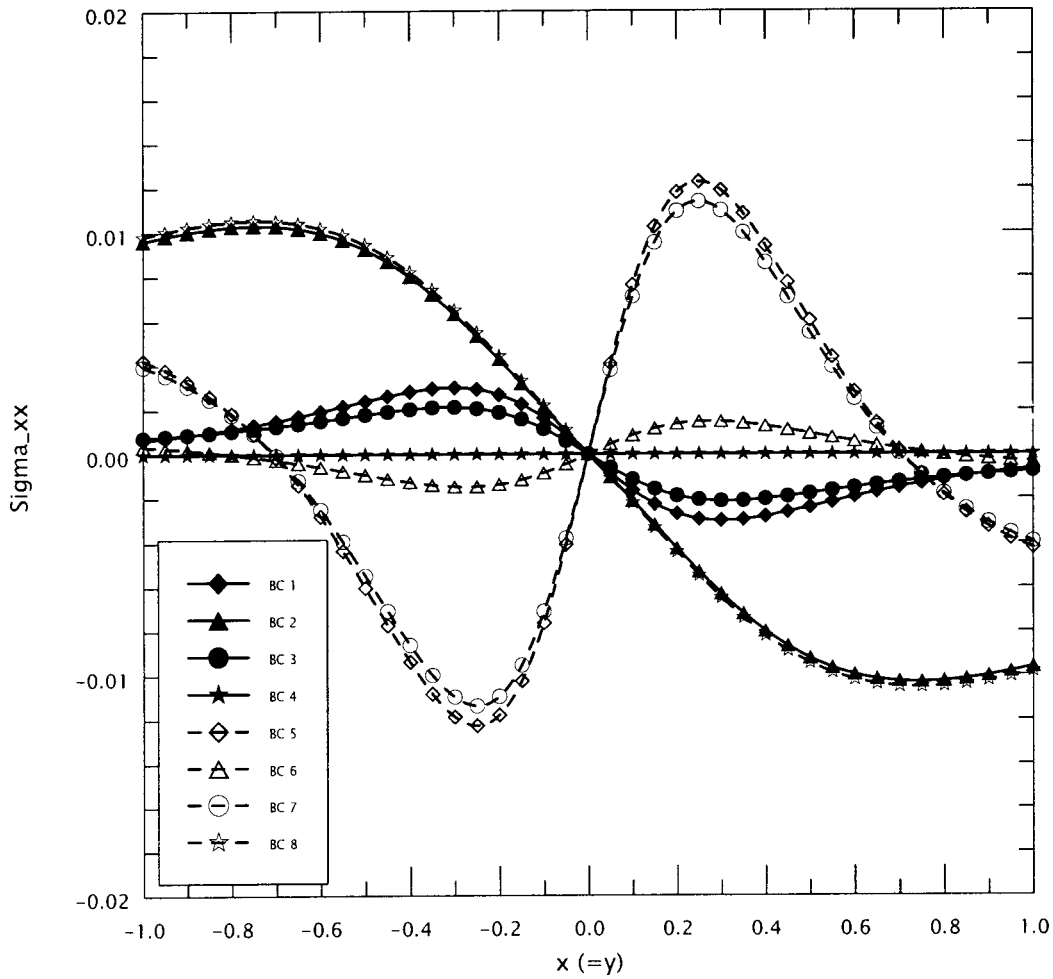

Fig. 3 Variation of in-plane stress component σ_{xx} along the line $x=y$ on the surface $z=0$, caused by the point force f=(1,0,0) at d=(0,0,1). Labels BC 1 to BC 8 correspond to the eight different sets of boundary conditions (2*a*–*h*).

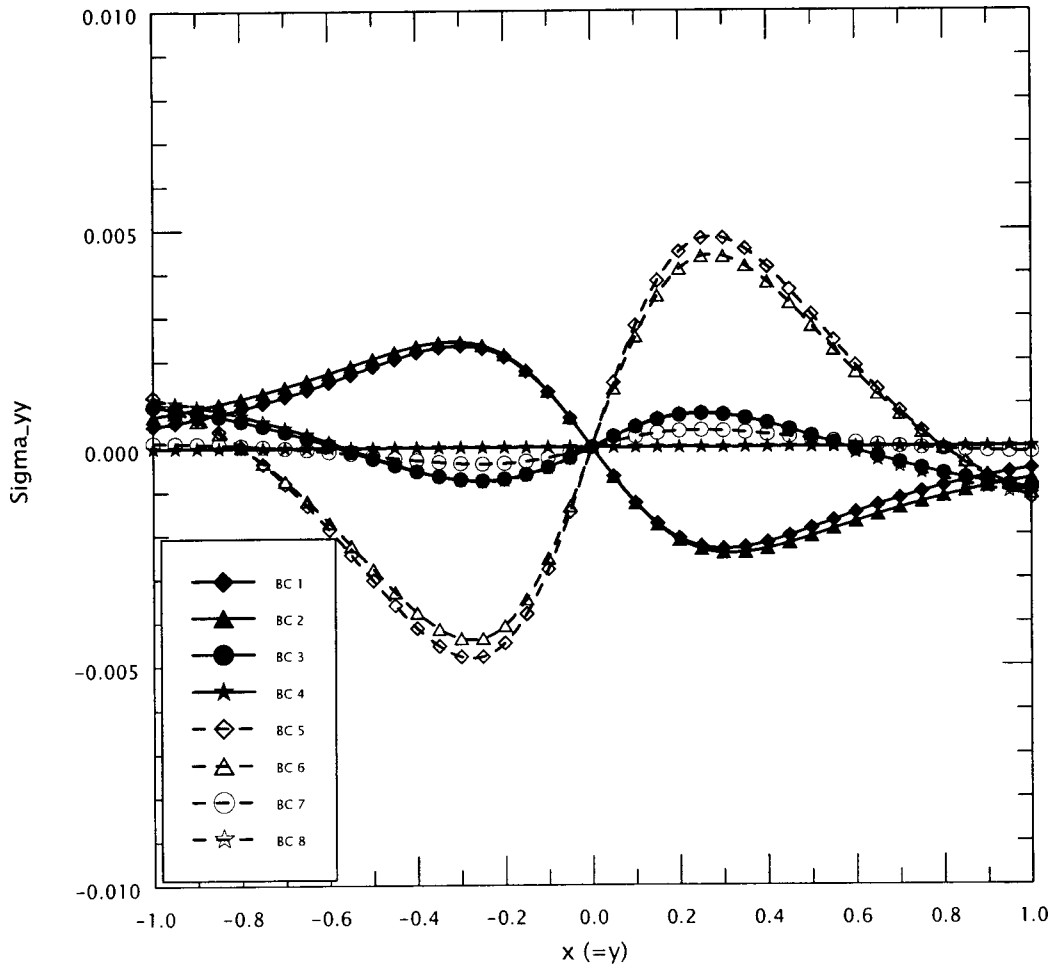

Fig. 4 Variation of in-plane stress component σ_{yy} along the line $x=y$ on the surface $z=0$, caused by the point force f=(1,0,0) at d=(0,0,1). Labels BC 1 to BC 8 correspond to the eight different sets of boundary conditions (2*a*–*h*).

symmetric (Figs. 3 and 4), a general feature also associated with the Mindlin solution in an isotropic half-space with traction-free boundary conditions.

2. The effect of material anisotropy on the surface normal stresses can be clearly see by comparing Fig. 1 to Fig. 2. For BC 1 and BC 5, both normal stresses σ_{xx} and σ_{yy} should be the same if the material is isotropic. However, the magnitudes are much different in the orthotropic half space for σ_{xx} and σ_{yy} under boundary condition BC 1 or BC 5.

3. It is of particular interest to order the normal stresses σ_{xx} and σ_{yy} at the surface point $\mathbf{x}=\mathbf{0}$, i.e., the symmetric point) from the largest tension (maximum) to the largest compression (minimum) according to the different sets of boundary conditions. While for those in Fig. 1, the descent order is BC 1, BC 3, BC 4, BC 2, BC 8, BC 6, BC 7, and BC 5, for those in Fig. 2, it is BC 1, BC 2, BC 4, BC 7, BC 3, BC 8, BC 6, and BC 5. It is observed that the boundary condition case BC 4 (Eq. (2*d*)) is in neutral for which the normal stresses σ_{xx} and σ_{yy} along the line $x=y$ on the surface are zero. While BC 1 and BC 3 predict a tensile and BC 2, BC 5–8 a compressive value for the normal stress σ_{xx}, BC 1 and BC 2 predict a tensile and BC 3, BC 5–8 a compressive value for the normal stress σ_{yy}.

Conclusions

In this paper, the complete set of three-dimensional Green's functions (displacements, stresses, and derivatives of displacements and stresses with respect to the source points), due to a point force in an anisotropic half-space with general boundary conditions, also called the generalized Mindlin solutions, are derived for the first time. Applying the Mindlin's superposition method, the half-space Green's function is obtained as a sum of the generalized Kelvin solution (Green's function in an anisotropic infinite space) and a Mindlin's complementary solution. While the generalized Kelvin solution is in an explicit form, the Mindlin's complementary part is expressed in terms of a simple line-integral over $[0,\pi]$. To handle the eight different sets of boundary conditions, a new matrix **K**, a combination of the eigenmatrices **A** and **B**, has been introduced so that the Green's functions corresponding to the eight different sets of boundary conditions can be expressed in a unified form, including the existing traction-free and rigid boundaries as the special cases.

The corresponding generalized Boussinesq solutions (for source point on the surface) and the special surface Green's functions (for both the source and field points on the surface) have been studied in details. In particular, it has been proved that under the general boundary conditions studied in this paper, the generalized Boussinesq solution is still well-defined, along with a physical explanation in terms of the equivalent concept of the Green's functions due to a point force and an infinitesimal dislocation loop.

A typical numerical example has been also presented for the Green's functions in an orthotropic half-space with the eight different sets of boundary conditions. The new numerical result illustrates clearly the effect of the boundary conditions, as well as material anisotropy, on the half-space Green's stresses. It is be-

lieved that the present complete Green's function solutions should be of interest to various boundary/contact designs and of particular value to various mechanical engineering and quantum device analyses based upon the integral equation method using Green's function.

Acknowledgments

The author would like to thank Prof. C. Q. Ru of the University of Alberta for discussions during the course of this study and the reviewer for his constructive comments, which lead to improvements of the earlier version of this article.

References

[1] Barber, J. R., 1992, *Elasticity*, Kluwer Academic Publishers, Dordrecht, The Netherlands.
[2] Ting, T. C. T., 1996, *Anisotropic Elasticity*, Oxford University Press, Oxford, UK.
[3] Davis, R. O., and Selvadurai, A. P. S., 1996, *Elasticity and Geomechanics*, Cambridge University Press, Cambridge, MA.
[4] Barnett, D. M., and Lothe, J., 1975, ''Line Force Loadings on Anisotropic Half-Spaces and Wedges,'' Phys. Norv., **8**, pp. 13–22.
[5] Mura, T., 1987, *Micromechanics of Defects in Solids*, 2nd Ed., Martinus Nijhof, Dordrecht, The Netherlands.
[6] Vlassak, J. J., and Nix, W. D., 1994, ''Measuring the Elastic Properties of Anisotropic Materials by Means of Indentation Experiments,'' J. Mech. Phys. Solids, **42**, pp. 1223–1245.
[7] Liao, J.J., and Wang, C. D., 1998, ''Elastic Solutions for a Transversely Isotropic Half-Space Subjected to a Point Load,'' Int. J. Numer. Analyt. Meth. Geomech., **22**, pp. 425–447.
[8] Wang, C. D., and Liao, J. J., 1999, ''Elastic Solutions for a Transversely Isotropic Half-Space Subjected to Buried Asymmetric-Loads,'' Int. J. Numer. Analyt. Meth. Geomech., **23**, pp. 115–139.
[9] Willis, J. R., 1966, ''Hertzian Contact of Anisotropic Bodies,'' J. Mech. Phys. Solids, **14**, pp. 163–176.
[10] Gladwell, G. M. L., 1980, *Contact Problems in the Classical Theory of Elasticity*, Sithoff and Noordhoff, The Netherlands.
[11] Barber, J. R., and Ciavarella, M., 2000, ''Contact Mechanics,'' Int. J. Solids Struct. **37**, pp. 29–43.
[12] Yu, H. Y., 2001, ''A Concise Treatment of Indentation Problems in Transversely Isotropic Half Spaces,'' Int. J. Solids Struct., **38**, pp. 2213–2232.
[13] Mindlin, R. D., 1936, ''Force at a Point in the Interior of a Semi-Infinite Solid,'' Physics (N.Y.), **7**, pp. 195–202.
[14] Pan, Y. C., and Chou, T. W., 1979, ''Green's Function Solutions for Semi-Infinite Transversely Isotropic Materials,'' Int. J. Eng. Sci. **17**, pp. 545–551.
[15] Barber, J. R., and Sturla, F. A., 1992, ''Application of the Reciprocal Theorem to Some Problems for the Elastic Half-Space'' J. Mech. Phys. Solids, **40**, pp. 17–25.
[16] Wu, K. C., 1998, ''Generalization of the Stroh Formalism to 3-Dimensional Anisotropic Elasticity,'' J. Elast., **51**, pp. 213–225.
[17] Pan, E., and Yuan, F. G., 2000, ''Three-Dimensional Green's Functions in Anisotropic Bimaterials,'' Int. J. Solids Struct., **37**, pp. 5329–5351.
[18] Yu, H. Y., Sanday, S. C., Rath, B. B., and Chang, C. I., 1995, ''Elastic Fields due to Defects in Transversely Isotropic Half Spaces,'' Proc. R. Soc. London, Ser. A, **A449**, pp. 1–30.
[19] Dundurs, J., and Hetenyi, M., 1965, ''Transmission of Force Between Two Semi-Infinite Solids,'' ASME J. Appl. Mech., **32**, pp. 671–674.
[20] Fabrikant, I., 1989, *Applications of Potential Theory in Mechanics: A Selection of New Results*, Kluwer Academic Publishers, Dordrecht, The Netherlands.
[21] Fabrikant, V. I., 1991, *Mixed Boundary Value Problems of Potential Theory and Their Applications in Engineering*, Kluwer Academic Publishers, Dordrecht, The Netherlands.
[22] Craig, R. F., 1992, *Soil Mechanics*, 5th Ed., Chapman & Hall, New York.
[23] Timoshenko, S., and Woinowsky-Krieger, S., 1987 *Theory of Plates and Shells*, 2nd Ed., McGraw-Hill, New York.
[24] Shilkrot, L. E., and Srolovitz, D. J., 1998, ''Elastic Analysis of Finite Stiffness Bimaterial Interfaces: Application to Dislocation-Interface Interactions,'' Acta Mater., **46**, pp. 3063–3075.
[25] Gharpuray, V. M., Dundurs, J., and Keer, L. M., 1991, ''A Crack Terminating at a Slipping Interface Between Two Materials,'' ASME J. Appl. Mech., **58**, pp. 960–963.
[26] Davies, J. H., and Larkin, I. A., 1994, ''Theory of Potential Modulation in Lateral Surface Superlattices,'' Phys. Rev. B, **B49**, pp. 4800–4809.
[27] Larkin, I. A., Davies, J. H., Long, A. R., and Cusco, R., 1997, ''Theory of Potential Modulation in Lateral Surface Superlattices, II. Piezoelectric Effect,'' Phys. Rev. B, **B56**, pp. 15,242–15,251.
[28] Holy, V., Springholz, G., Pinczolits, M., and Bauer, G., 1999, ''Strain Induced Vertical and Lateral Correlations in Quantum Dot Superlattices,'' Phys. Rev. Lett., **83**, pp. 356–359.
[29] Ru, C. Q., 1999, ''Analytic Solution for Eshelby's Problem of an Inclusion of Arbitrary Shape in a Plane or Half-Plane,'' ASME J. Appl. Mech., **66**, pp. 315–322.
[30] Ru, C. Q., 2000, ''Eshelby's Problem for Two-Dimensional Piezoelectric Inclusion of Arbitrary Shapem,'' Proc. R. Soc. London, Ser. A, **A456**, pp. 1051–1068.
[31] Eshelby, J. D., 1957, ''The Determination of the Elastic Field on an Ellipsoidal Inclusion, and Related Problems,'' Proc. R. Soc. London, Ser. A, **A241**, pp. 376–396.
[32] Ting, T. C. T., 2000, ''Recent Developments in Anisotropic Elasticity,'' Int. J. Solids Struct., **37**, pp. 401–409.
[33] Ting, T. C. T., 2001, ''The Wonderful World of Anisotropic Elasticity—An Exciting Theme Park to Visit,'' *Proc. 4th Pacific International Conference on Aerospace Science and Technology*,'' pp. 1–7.
[34] Ting, T. C. T., and Wang, M. Z., 1992, ''Generalized Stroh Formalism for Anisotropic Elasticity for General Boundary Conditions,'' Acta Mech. Sin., **8**, pp. 193–207.
[35] Wang, M. Z., Ting, T. C. T., and Yan, G., 1993, ''The Anisotropic Elastic Semi-Infinite Strip,'' Q. Appl. Math., **51**, pp. 283–297.
[36] Tewary, V. K., 1995, ''Computationally Efficient Representation for Elastostatic and Elastodynamic Green's Functions,'' Phys. Rev. B, **51**, pp. 15,695–15,702.
[37] Ting, T. C. T., and Lee, V. G., 1997, ''The Three-Dimensional Elastostatic Green's Function for General Anisotropic Linear Elastic Solids,'' Q. J. Mech. Appl. Math., **50**, pp. 407–426.
[38] Sales, M. A., and Gray, L. J., 1998, ''Evaluation of the Anisotropic Green's Function and its Derivatives,'' Comput. Struct., **69**, pp. 247–254.
[39] Tonon, F., Pan, E., and Amadei, B., 2001, ''Green's Functions and Boundary Element Method Formulation for 3D Anisotropic Media,'' Comput. Struct., **79**, pp. 469–482.
[40] Pan, E., 1997, ''A General Boundary Element Analysis of 2-D Linear Elastic Fracture Mechanics,'' Int. J. Fract., **88**, pp. 41–59.
[41] Pan, E., 2002, ''Three-Dimensional Green's Functions in Anisotropic Magneto-Electro-Elastic Bimaterials,'' J. Appl. Math Phys., pp. 815–838.
[42] Walker, K. P., 1993, ''Fourier Integral Representation of the Green's Function for an Anisotropic Elastic Half-Space,'' Proc. R. Soc. London, Ser. A, **A443**, pp. 367–389.
[43] Love, A. E. H., 1994, *A Treatise on the Mathematical Theory of Elasticity*, 4th Ed., Dover Publication, New York.
[44] Sokolnikoff, I. S., 1956, *Mathematical Theory of Elasticity*, McGraw-Hill, New York.
[45] Hirth, J. P., and Lothe, J., 1982, *Theory of Dislocations*, 2nd Ed., John Wiley and Sons, New York.
[46] Pan, E., 1991, ''Dislocation in an Infinite Poroelastic Medium,'' Acta Mech., **87**, pp. 105–115.
[47] Paget, D. F., 1981, ''The Numerical Evaluation of Hadamard Finite-Part Intervals,'' Numer. Math., **36**, pp. 447–453.
[48] Monegato, G., 1994, ''Numerical Evaluation of Hypersingular Integrals,'' J. Comput. Appl. Math., **50**, pp. 9–31.
[49] Mastronardi, N., and Occorsio, D., 1996, ''Some Numerical Algorithms to Evaluate Hadamard Finite-Part Integrals,'' J. Comput. Appl. Math., **70**, pp. 75–93.
[50] Pan, E., and Yang, B., 2003, ''Three-Dimensional Interfacial Green's Functions in Anisotropic Bimaterials,'' Appl. Math. Model., in press.